instead of two times, larger than those of Cu_8O, which indicates that the expansion of the $Cu_{64}O$ lattice due to the interstitial O atoms in the Cu lattice is less than that in Cu_8O. It is possible that such a strain may cause distortions of the substrate metal and if the strain is large enough it will result in a separation of the 'oxidized' part from the matrix and produce a large number of very small and thin slightly 'oxidized' crystallites. This may be one of the reasons why Cu_8O can be more easily found than $Cu_{64}O$ during observation in the electron microscope. It may be noted that, for the suboxides with very low oxygen content, the structure images cannot be obtained from a very thin crystal, *i.e.* the weak phase object condition, but can be obtained from a thicker specimen in the dynamic scattering object condition. On increasing the thickness of the crystal to more than a certain critical thickness, the contrast of the images of the heavy atoms decreases and that of the light atoms increases. Thus at some optimum thickness of the crystal, the images of the light atoms can be observed as well as those of the heavy atoms. Thus the dynamical scattering of electron waves can be used effectively for the structure analysis of the crystals containing light atoms.

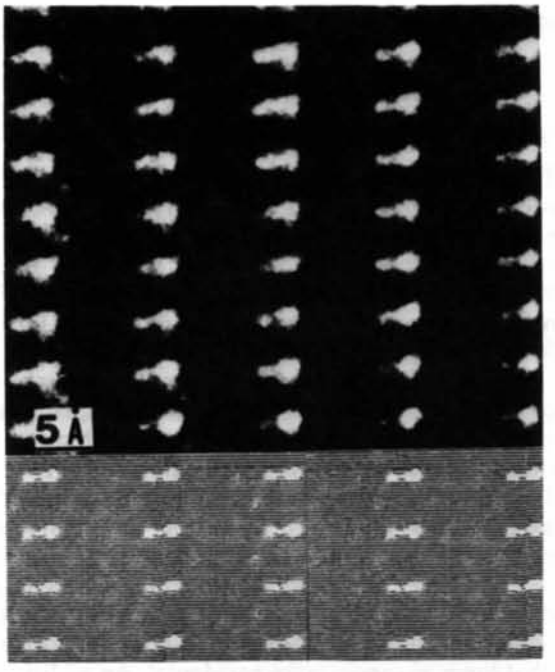

Fig. 17. Comparison of the observed and calculated images of $Cu_{64}O$. The magnified images on the top, taken from the encircled area *C* in Fig. 4, match the calculated ones (bottom) obtained with the value of defocus of $\Delta f = -500$ Å and thickness of $t = 670 \sim 700$ Å.

The authors would like to record their thanks to Mr B. S. Zou and Drs H. Endoh, M. Tomita and N. Ajika for their help in the experiments and to Mr Y. K. Wu, and Professors G. Thomas and S. Suryanarayana for helpful discussions.

References

DAHMEN, U. & THOMAS, G. (1979). *Scr. Metall.* **13**, 527–530.
GUAN, R., HASHIMOTO, H. & KUO, K. H. (1984). *Acta Cryst.* B**40**, 560–566.
GUAN, R., HASHIMOTO, H. & YOSHIDA, T. (1984). *Acta Cryst.* B**40**, 109–114.
HAHN, T. (1983). Editor. *International Tables for Crystallography*, Vol. *A*, pp. 56–57, 234–235.
KHACHATURYAN, A. G. (1983). *Theory of Structural Transformations in Solids.* New York: John Wiley.

Acta Cryst. (1985). B**41**, 225–230

A Combined X-ray and Neutron Diffraction Study of Bi_3ReO_8; a New Structure Type Based on Fluorite

BY A. K. CHEETHAM* AND A. R. RAE SMITH

Department of Chemical Crystallography, University of Oxford, 9 Parks Road, Oxford OX1 3PD, England

(*Received* 21 *October* 1984; *accepted* 6 *February* 1985)

Abstract

The fluorite-related crystal structure of Bi_3ReO_8 has been solved by a combination of X-ray and neutron diffraction techniques. The lattice is cubic, $a = 11{\cdot}590\,(1)$ Å, space group $P2_13$, $Z = 8$. The final *R* factors from the neutron powder study were $R_I = 5{\cdot}3\%$, $R_P = 10{\cdot}4\%$. The principal deviation from the ideal fluorite structure is found in the ReO_4 tetrahedra, which are rotated 40° about the ⟨111⟩ direction in order to accommodate the stereochemical activity of the Bi lone pairs. The relationship of the structure to those of the related rare-earth compounds, Ln_3ReO_8, is discussed.

* Author to whom correspondence should be addressed.

0108-7681/85/040225-06$01.50

Introduction

We have described the preparation and characterization of Bi_3ReO_8 in previous papers on our investigation of the Bi–Re–O system (Cheetham & Rae Smith, 1981; Rae Smith & Cheetham, 1979). It is the most stable compound in the Bi_2O_3-Re_2O_7 system, possessing no appreciable range of composition and melting above 1473 K, and is the sole product obtained when phases containing more than 25% Re_2O_7 are heated in air above 873 K. Colourless crystals may be grown by vapour transport at 1073 K from reaction mixtures of ReO_3 and Bi_2O_3 (the other major product being $BiRe_2O_6$). The polycrystalline material has a very pale cream colour.

In this paper we describe the determination of the crystal structure. The space group and metal-atom positions were derived from a combination of single-crystal and powder X-ray diffraction data, but because of the high pseudosymmetry of the metal-atom positions, the O atoms could not be located. A powder neutron diffraction study allowed a choice to be made between the various models, leading to the complete determination of the structure.

Experimental

The X-ray powder diffraction data were collected on a Philips X-ray powder diffractometer using Cu $K\alpha$ radiation. The diffracted intensity was measured to a 2θ limit of 85° with a step size of 0·01°. A high monitor count was used to ensure good statistics for the weak superlattice reflections. The data yielded a total of 72 resolved peaks corresponding to 186 independent reflections.

The X-ray single-crystal data were collected on an Enraf-Nonius CAD-4F diffractometer using Mo $K\alpha$ radiation. Intensities of 2345 reflections were collected to a θ limit of 30°. After applying Lorentz and polarization corrections, equivalent reflections were merged to yield 433 reflections with $I/\sigma(I) > 2$. The crystal was small (average diameter 0·1 mm) and multi-faceted, with the prominent {110} faces giving the crystal a rhombic dodecahedral appearance. This made the application of the necessary absorption correction (de Meulenaer & Tompa, 1965) (μ = 910 cm^{-1}) extremely difficult, and attempts to do so were unsatisfactory.

The neutron powder data were collected on the D1A high-resolution powder diffractometer at the ILL, Grenoble. The diffracted intensity was measured to a 2θ limit of 150° with a step size of 0·05°, using a neutron wavelength of 1·511 Å. The sample (8 g of polycrystalline Bi_3ReO_8) was contained in a vanadium can.

X-ray calculations were carried out using the Oxford *CRYSTALS* package (Carruthers, 1978) for the single-crystal data and a local program (Wiseman, 1974) for the analysis of powder intensity data. Calculations on the neutron powder data used an interactive version of the Rietveld profile refinement program (Rae Smith, Cheetham & Skarnulis, 1979). All values for X-ray scattering factors and anomalous-dispersion coefficients were taken from *International Tables for X-ray Crystallography* (1974). Values of 9·2, 8·6 and 5·8 fm were taken for the neutron scattering lengths of Re, Bi and O respectively.

Determination of the structure

Determination of the space group

The X-ray diffraction data showed that the lattice was cubic, with cell parameter $a = 11{\cdot}590\ (1)$ Å, and the intensity distribution indicated a relationship to the fluorite structure with $a = 2a_F$, where a_F is the cell parameter of the face-centred fluorite subcell. For convenience we shall refer to those reflections indexable on the fluorite subcell ($h/2$, $k/2$, $l/2$ all even or all odd) as sublattice reflections, and the remaining weaker reflections as superlattice reflections. The ratio of the X-ray intensities of the strongest sublattice to the most intense superlattice reflection is 15:1.

The X-ray single-crystal data indicated that the Laue group was $m3$ ($I_{hlk} \neq I_{hkl}$) rather than $m3m$ and suggested the systematic absence condition $h00$, $h = 2n+1$. However, this class of reflections is very small and falls exclusively among the weaker superlattice reflections, and so we could not discount the possibility that these absences were accidental. An additional feature of the data is that all the stronger superlattice reflections obey the condition $h+k+l = 2n$, implying that the large cell is approximately body-centred.

Examination of the infrared spectrum of Bi_3ReO_8 narrowed down the choice of space groups. The spectrum (see Fig. 1) shows intense peaks around

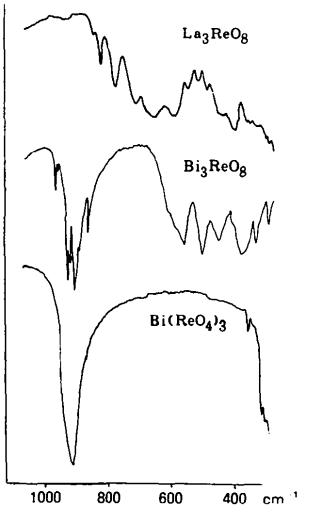

Fig. 1. Infrared spectra of La_3ReO_8, Bi_3ReO_8 and $Bi(ReO_4)_3$.

900 cm^{-1}, characteristic of tetrahedrally coordinated Re^{VII} as found in the perrhenates (Busey & Keller, 1964; Ulbricht & Kreigsmann, 1968) and illustrated in Fig. 1 by the spectrum of $Bi(ReO_4)_3$. These peaks are absent in compounds such as La_3ReO_8 that contain octahedrally coordinated Re^{VII}. The presence of approximately tetrahedral ReO_4 units in an ordered structure limits the point group to 23 and the space groups to $P23$ and $P2_13$, with the body-centred groups $I23$ and $I2_13$ giving close approximations. The systematic absence condition favours $P2_13$, but for the reasons described above, $P23$ must also be taken into consideration.

Determination of the metal-atom positions

Preliminary calculations using the X-ray powder data indicated that the metal-atom positions were slightly displaced from the ideal fluorite positions, since merely ordering the Re and Bi atoms on the metal sites did not generate sufficient superlattice intensity. The calculations also showed that the required displacements were quite small (<0·35 Å).

Three types of Patterson function were calculated from the single-crystal data: a standard Patterson function employing all reflections, a sharpened Patterson function, and a Patterson function based on the superlattice reflections alone. The small values of the displacements combined with the high lattice symmetry resulted in broad metal-metal vectors in the Patterson functions, and made it impossible to deduce anything about the ordering of the atoms or the nature of the displacements. Direct methods were also tried, but met with no success. This is doubtless due to the high lattice symmetry and the pseudosymmetry of the metal-atom positions, together with the noncentrosymmetric nature of the structure.

The positions of the symmetry elements in the space groups $P23$ and $P2_13$ lead in each case to four possible models for ordering the metal atoms. The ideal positions for these models may be derived by placing the Re atoms on the body diagonal of the large cubic cell at positions (0, 0, 0), $(\frac{1}{4}, \frac{1}{4}, \frac{1}{4})$, $(\frac{1}{8}, \frac{1}{8}, \frac{1}{8})$ or $(\frac{3}{8}, \frac{3}{8}, \frac{3}{8})$, and on the body-centred related positions. These we shall term models (1)-(4), respectively, in each space group. The Re positions are fourfold (x, x, x) positions except for model $P23$-(1) which contains a combination of two invariant sites for the Re atom: (0, 0, 0) and the threefold position $(\frac{1}{2}, 0, 0)$. The Bi atoms occupy the remaining sites in the face-centred array. These models are illustrated in Fig. 2. The metal ordering in models (1) and (2) can be described in terms of the fluorite subcell as that found in Cu_3Au and other alloys, while the metal ordering in models (3) and (4) requires a description in terms of the larger cell. Models $P23$-(3) and $P23$-(4) have the chemically unsatisfactory feature of Re_4O coordination clusters.

Table 1. *Summary of X-ray refinements of metal-atom positions*

	R factors (R_F) (%)			
Model	(1)	(2)	(3)	(4)
$P23$	16·1	13·5	15·7	17·4
$P2_13$	16·4	18·6	12·9	21·2

Metal-atom positions [model $P2_13$-(3)] used as starting positions in neutron calculations

	x	*y*	*z*
Re(1)	0·108	0·108	0·108
Re(2)	0·602	0·602	0·602
Bi(1)	0·095	0·365	0·356
Bi(2)	0·133	0·112	0·624

We then resorted to trial-and-error methods. For each model, the metal atoms were displaced from their ideal positions and the atomic positional coordinates refined. The initial displacements were varied until a set was found that converged to a minimum in less than four cycles of refinement. The powder data proved more stable in refinement using this technique, and were used to obtain the optimum displacements in each of the eight models. These values were then refined together with individual anisotropic thermal parameters using the single-crystal data. The final *R* factors (based on structure factors, $R_F = 100 \sum |F_o - F_c| / \sum F_o$) are shown in Table 1. Disappointingly, there is no great preference for any one model, although $P2_13$-(3) and $P23$-(2) have the lowest values. Examination of the data showed that they suffered severely from extinction and absorption. While the complex shape of the crystal led to a lack of success in correcting for absorption, application of an extinction correction lowered the *R* factors by 3% from the values shown in Table 1.

Because of the high pseudosymmetry of the metal-atom positions, it was important to establish that the models had not refined to false minima. To examine this possibility, a series of *R*-factor maps was calculated for each model. Each positional parameter was allowed to vary in nine steps with initial bounds of ±0·08 from the ideal position. The step size was decreased when minima were found. The *R* factor

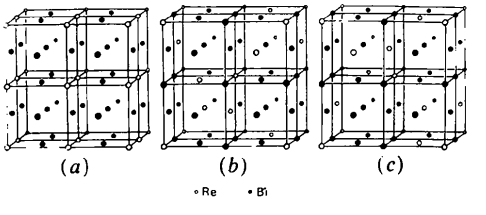

Fig. 2. Metal-atom models for Bi_3ReO_8. (*a*) $P23$-(1), $P23$-(2), $P2_13$-(1), $P2_13$-(2). (*b*) $P23$-(3). (*c*) $P2_13$-(3). For the sake of comparison all models have been shown with the Re atom at (x, x, x) at the bottom left corner of each diagram. Models $P23$-(4) and $P2_13$-(4) may be derived from models $P23$-(3) and $P2_13$-(3) respectively by inverting the metal ordering through the centre of the large cube in the diagram.

was calculated from 80 reflections using the powder intensity data, and a Fortran program was written to minimize the calculation involved. A typical computation time for 4×10^5 R factors varying all 8 parameters was 120 s on a CDC 7600 computer. The results of these calculations confirmed that the positions found by trial and error were in fact the lowest minima in each map.

Determination of the O*-atom positions*

Difference Fourier calculations based on the eight models for the metal-atom positions failed to reveal any O-atom positions that were both acceptable and stable on refinement, but a re-examination of the Patterson maps revealed a small but distinct peak at (0, −0·064, 0·139) in maps derived from powder as well as single-crystal data. This peak is at a distance of 1·77 Å from the origin and has the correct height for a Re–O vector (55 based on an origin peak of 999). Although it is unusual to see metal–O vectors in Patterson functions of structures containing such large heavy-metal atoms ($Z_{Re}=75$, $Z_{Bi}=83$), the vector length is typical of that found in compounds containing tetrahedral ReO_4 groups. Moreover, it makes an angle of 106·4° (approximately tetrahedral) with the [111] direction. It is considerably displaced from the vector that would be observed if the O atom was simply drawn towards Re from the ideal fluorite position in order to make a sensible Re–O bond length (0·088, −0·088, 0·088). The displacement corresponds to a rotation of 40° about the [111] direction.

O tetrahedra were then placed around the Re positions in each model, using the vector found in the Patterson map and placing the fourth O of each tetrahedron on the threefold axis. However, the O positions were not stable on refinement in any of the models, nor did they help to reveal any remaining O-atom positions in difference Fourier maps. While this situation was unsatisfactory, it was not totally unexpected. If the major distortion of the structure occurs in the O sublattice (as is apparent from the large rotation of the ReO_4 tetrahedra), the relative contribution of the O atoms to the superlattice reflections is much greater than that expected from a consideration of the relative scattering lengths of Bi, Re and O. Thus unless the O-atom positions are known with reasonable precision, the Fourier functions will not be phased correctly. We therefore attempted to solve the structure from neutron powder diffraction data, since with neutron radiation the O atoms represent the major scattering material in the unit cell, having a contribution of 57% compared to the corresponding value of 16% for X-rays.

Two points emerge immediately from a comparison of the X-ray and neutron powder scans (Fig. 3). First, the deduction made above, that the major distortion is in the O sublattice, is clearly justified, since the intensity ratio of the most intense sublattice to the most intense superlattice reflection is now 2:1 compared to the X-ray value of 15:1. Second, the approximate body-centring of the large cell is even more apparent in the neutron data, allowing preliminary calculations to be carried out in the body-centred space groups.

The R-factor-map technique described above was used to identify suitable starting positions for the O atoms in later refinement; 41 intensities, corresponding to 79 reflections, were used in these calculations. The metal atoms were placed in the positions determined from the X-ray analyses and the O atoms in the ReO_4 tetrahedra were placed on the positions derived from the X-ray Patterson vector. This left half of the O-atom positions to be found. The number of parameters was limited to four in most cases by carrying out the calculations in the body-centred space group. This allowed a larger range of positions for the O atoms to be searched. The displacements were centred about ideal fluorite positions.

Two models, $P2_13$-(1) and $P2_13$-(3), gave sets of positions with R factors of less than 25%, and these were then used in the profile refinement. Initially, refinement was carried out on a limited range of data ($0<2\theta<50°$) corresponding to that used for the R-factor-map calculations. Both models refined to give good fits, but when the data were extended to $2\theta=150°$, it was clear that while model $P2_13$-(3) fitted very well over the whole profile, $P2_13$-(1) fitted poorly

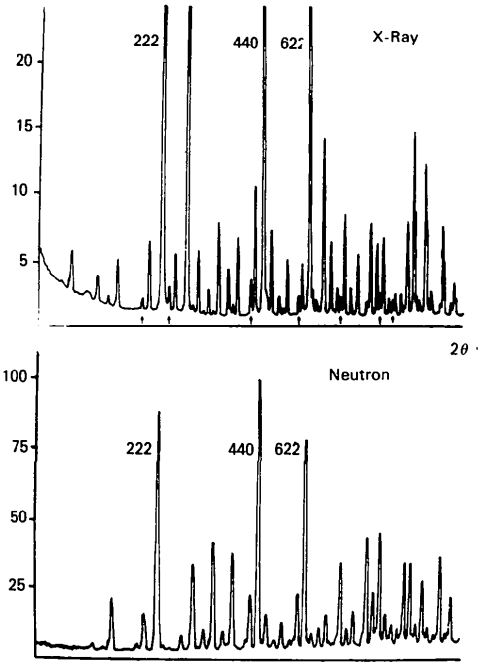

Fig. 3. Comparison of X-ray and neutron scans. Intensities have been scaled to a value of 100 for the maximum intensity observed in each scan. The arrows under the X-ray scan show relatively strong reflections with $h+k+l=2n+1$.

Table 2. *Structural data for* Bi_3ReO_8 (*e.s.d.'s in parentheses*)

	Site	x	y	z
Re(1)	4(*a*)	0·1192 (3)	0·1192 (3)	0·1192 (3)
Re(2)	4(*a*)	0·6192 (3)	0·6192 (3)	0·6192 (3)
Bi(1)	12(*b*)	0·1448 (3)	0·3513 (3)	0·3890 (3)
Bi(2)	12(*b*)	0·1193 (3)	0·1530 (3)	0·6308 (3)
O(1)	4(*a*)	0·0323 (6)	0·0323 (6)	0·0323 (6)
O(2)	4(*a*)	0·5319 (6)	0·5319 (6)	0·5319 (6)
O(3)	12(*b*)	0·1391 (5)	0·2543 (5)	0·0570 (5)
O(4)	12(*b*)	0·6163 (6)	0·7589 (5)	0·5674 (5)
O(5)	4(*a*)	0·2911 (5)	0·2911 (5)	0·2911 (5)
O(6)	4(*a*)	0·7797 (5)	0·7797 (5)	0·7797 (5)
O(7)	12(*b*)	0·2329 (5)	0·2140 (4)	0·4935 (6)
O(8)	12(*b*)	0·2605 (6)	0·5399 (4)	0·0019 (6)

B_{Re} 0·79(4)Å^2. B_{Bi} 1·10(3)Å^2. B_O 1·68(3)Å^2

above $2\theta = 50°$. When interatomic distances and angles were calculated, model $P2_13$-(1) could be safely rejected since it gave an unacceptably low O–O contact of 1·6 Å and metal-O coordinations that were chemically unreasonable. Model $P2_13$-(3), however, gave good metal coordination geometries and a closest O–O contact of 2·60 Å. Subsequent calculations on model $P2_13$-(3) refining all positional parameters, three thermal parameters (one for each atomic type), and the instrumental parameters gave an R factor (based on intensities, $R_I = 100 \sum |I_o - I_c| / \sum I_o$) of 5·3% and a profile R factor ($R_p = 100 \sum |y_o - y_c| / \sum y_o$) of 10·4%. There were no major discrepancies in the calculated profile (Fig. 4).

As a final test, the positions determined from the neutron profile refinement were used in a refinement of the X-ray powder data (which do not suffer from the severe extinction associated with the single-crystal data). After two cycles of refinement of a scale factor and an overall thermal parameter, the R factor (based on intensities) was 5·8%. Because of the severe absorption, the overall thermal parameter refined to a negative value ($B = -3·0$ Å^2). In subsequent cycles of refinement, the metal-atom positions did not shift by more than one e.s.d., although the O-atom positions, as previously, were unstable.

Table 3. *Selected distances* (Å) *and angles* (°) (*e.s.d.'s* 0·008 Å *and* 0·5°, *respectively*)

Re(1)–O(1)	1·746	Re(2)–O(2)	1·753
Re(1)–O(3) ×3	1·739	Re(2)–O(4) ×3	1·728
O(1)–Re(1)–O(3)	110·90	O(2)–Re(2)–O(4)	109·23
O(3)–Re(1)–O(3)	108·00	O(4)–Re(2)–O(4)	109·71
Bi(1)–O(8)	2·124	Bi(2)–O(8)	2·124
Bi(1)–O(5)	2·156	Bi(2)–O(6)	2·146
Bi(1)–O(7)	2·245	Bi(2)–O(7)	2·184
Bi(1)–O(7′)	2·575	Bi(2)–O(7′)	2·666
Bi(1)–O(8′)	2·628	Bi(2)–O(3)	2·843
O(8)–Bi(1)–O(5)	96·31	O(8)–Bi(2)–O(6)	100·81
O(8)–Bi(1)–O(7)	81·56	O(8)–Bi(2)–O(7)	80·49
O(8)–Bi(1)–O(7′)	83·79	O(8)–Bi(2)–O(7′)	72·16
O(8)–Bi(1)–O(8′)	98·80	O(8)–Bi(2)–O(3)	148·12
O(5)–Bi(1)–O(7)	72·36	O(6)–Bi(2)–O(7)	78·54
O(5)–Bi(1)–O(7′)	65·95	O(6)–Bi(2)–O(7′)	68·45
O(5)–Bi(1)–O(8′)	135·75	O(6)–Bi(2)–O(3)	106·76
O(7)–Bi(1)–O(7′)	133·69	O(7)–Bi(2)–O(7′)	131·37
O(7)–Bi(1)–O(8′)	69·14	O(7)–Bi(2)–O(3)	89·48
O(7′)–Bi(1)–O(8′)	156·90	O(7′)–Bi(2)–O(3)	133·12

The structural data are summarized in Table 2, and illustrated in Figs. 5 and 6. Table 3 contains selected interatomic distances and angles.

Discussion

The structure of Bi_3ReO_8 contains an ordered array of ReO_4 tetrahedra in a distorted fluorite structure. The ReO_4 tetrahedra are slightly deformed, leading to the splitting of the peaks in the infrared spectrum at 900 cm^{-1}, but the bond distances (mean 1·74 Å) are in good agreement with those found in perrhenates. The tetrahedra cluster together, as can be seen from the projection down the ⟨111⟩ direction in Fig. 5. The Bi coordination is open, as found in the com-

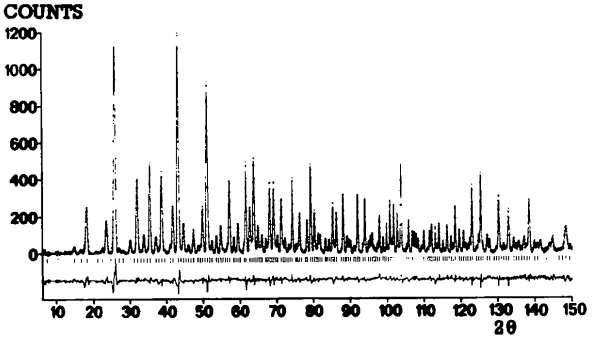

Fig. 4. Calculated (full line), observed (points) and difference profiles from the final refinement of the neutron data. Reflection positions are shown. [The numerical values of the profiles have been deposited with the British Library Lending Division as Supplementary Publication No. SUP42044 (21 pp.). Copies may be obtained through The Executive Secretary, International Union of Crystallography, 5 Abbey Square, Chester CH1 2HU, England.]

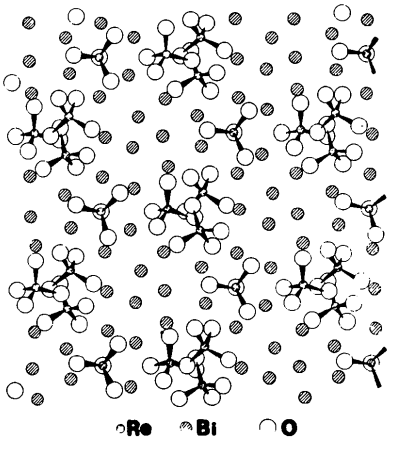

Fig. 5. Projection of the structure of Bi_3ReO_8 down ⟨111⟩. For clarity, only the O atoms in the ReO_4 tetrahedra are shown and only one of each pair of atoms related by the approximate body-centring is shown. The projected positions of the remaining O atoms lie near the Bi-atom positions.

pounds $BiReO_4$ and $BiRe_2O_6$, with three close O atoms (2·1 Å) and one [Bi(1)] or two [Bi(2)] further O atoms at 2·6 Å. The deviations from the ideal cubic coordination are shown in Fig. 7. The major distortion from the ideal fluorite structures comes from the O atoms in the ReO_4 tetrahedra (see Table 4).

The cell volume of Bi_3ReO_8 is about 25% larger than typical fluorite compounds ($a_F = 5{\cdot}8$ Å compared to $a_F = 5{\cdot}3$ Å for α-Er_3ReO_8). The metal-O distances in an undistorted fluorite structure of this size would be 2·5 Å. Since the ReO_4 tetrahedra, which account for 50% of the O atoms, have Re-O distances of 1·74 Å, one might have expected a slightly smaller volume. It is also difficult for the same reason to explain the rotation of the ReO_4 tetrahedra by 40° about [111] (see above). We were able to account for anomalies in volume in $BiReO_4$ and $BiRe_2O_6$ in terms of a stereochemically active Bi lone pair (Rae Smith & Cheetham, 1979), and vacant anion sites could be identified in both these structures to accommodate it. When the occupied volume in Bi_3ReO_8 is examined, there is a site about 1 Å from each Bi atom [for Bi(1) the approximate position is (0·314, 0·324, 0·102)] which could accommodate the lone pair. These sites are related to ideal fluorite anion sites [$(\frac{1}{4}, \frac{1}{4}, 0)$, *etc.*] by displacements of 1·6 Å towards the Bi atoms, and fall between the O atoms at the base of the ReO_4 tetrahedra.

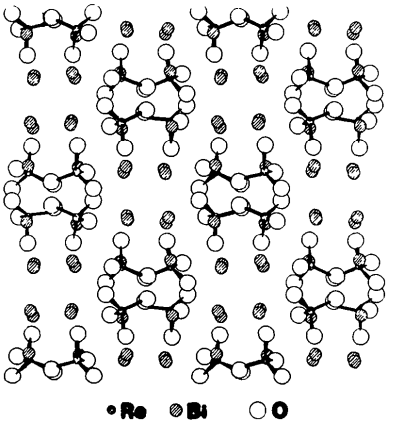

Fig. 6. Projection of the structure of Bi_3ReO_8 down ⟨100⟩. For clarity, only the O atoms in the ReO_4 tetrahedra are shown. The unit-cell origin is at the bottom left corner of the diagram.

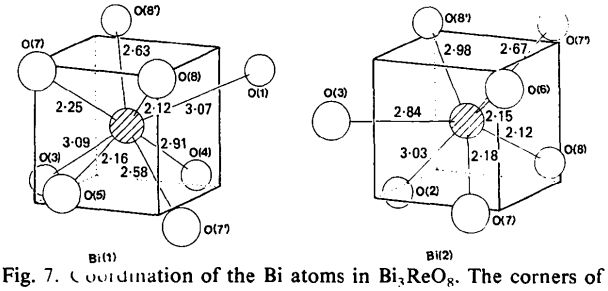

Fig. 7. Coordination of the Bi atoms in Bi_3ReO_8. The corners of each cube represent the positions of ideal fluorite coordination.

Table 4. *Deviations from ideal fluorite positions* (Å)

Re(1)	0·12	Re(2)	0·12
Bi(1)	0·39	Bi(2)	0·34
O(1)	0·65	O(2)	0·64
O(3)	1·45	O(4)	1·56
O(5)	0·83	O(6)	0·60
O(7)	0·47	O(8)	0·48

The structures of the closest analogues to Bi_3ReO_8, the rare-earth rhenium oxides Ln_3ReO_8, have all been determined and fall into two main types. The low-pressure α-form of Ln_3ReO_8 (Ln = Tb - Lu, Y) appears to be a disordered fluorite phase (Baud & Besse, 1974) and has a very small range of thermal stability (323 K), while the early rare-earth compounds [Ln = La (Baud, Besse, Chevalier & Gasperin, 1979; Rae Smith, Cheetham & Fuess, 1984), Ce - Gd (Besse, Bolte, Baud & Chevalier, 1976)] and the high-pressure β-form of the later rare-earth compounds [Ln = Tb - Lu, Y (Baud, Besse, Chevalier & Gasperin, 1981)] have closely related structures which can be described in terms of an ordered fluorite substructure. The early rare-earth compounds resemble Bi_3ReO_8 in their high thermal stability, but their structures are essentially different from Bi_3ReO_8 in that they contain octahedrally coordinated Re. Bi_3ReO_8 thus appears to have a unique structure.

We wish to thank Hermann Starck Berlin for the provision of rhenium, and the SERC for the provision of neutron and computing facilities.

One of us (ARRS) is pleased to acknowledge support through National Science Foundation Grant DMR 8108306 for the completion of this work.

References

BAUD, G. & BESSE, J.-P. (1974). *Mater. Res. Bull.* **9**, 1499-1502.

BAUD, G., BESSE, J.-P., CHEVALIER, R. & GASPERIN, M. (1979). *J. Solid State Chem.* **29**, 267-272.

BAUD, G., BESSE, J.-P., CHEVALIER, R. & GASPERIN, M. (1981). *J. Solid State Chem.* **38**, 186-191.

BESSE, J.-P., BOLTE, M., BAUD, G. & CHEVALIER, R. (1976). *Acta Cryst.* B**32**, 3045-3048.

BUSEY, R. H. & KELLER, O. L. (1964). *J. Chem. Phys.* **41**, 215-225.

CARRUTHERS, J. R. (1978). *CRYSTALS User Manual.* Oxford Univ. Computing Laboratory.

CHEETHAM, A. K. & RAE SMITH, A. R. (1981). *Mater. Res. Bull.* **16**, 7-14.

International Tables for X-ray Crystallography (1974). Vol. IV. Birmingham: Kynoch Press. (Present distributor D. Reidel, Dordrecht.)

MEULENAER, J. DE & TOMPA, H. (1965). *Acta Cryst.* **19**, 1014-1018.

RAE SMITH, A. R. & CHEETHAM, A. K. (1979). *J. Solid State Chem.* **30**, 345-352.

RAE SMITH, A. R. CHEETHAM, A. K. & FUESS, H. (1984). *Z. Anorg. Allg. Chem.* **510**, 46-50.

RAE SMITH, A. R. CHEETHAM, A. K. & SKARNULIS, A. J. (1979). *J. Appl. Cryst.* **12**, 485-486.

ULBRICHT, K. & KREIGSMANN, H. (1968). *Z. Anorg. Allg. Chem.* **358**, 193-209.

WISEMAN, P. J. (1974). DPhil Thesis, Oxford.